865

Effect of Some Physical Factors and Chemical Processing on the Yield and Quality of Nanosilica Derived from Rice Husk: Effectiveness of H3PO4 Pre-treatment on Structural and Optical Properties

[1]C. Mbakaan
[1]Dept Department of Science Laboratory Technology, Physics/Electronics Section,
Benue State Polytechnic, P.M.B. 01, Ugbokolo.

Article Info

ABSTRACT

The research reports the effect of location, fertilizer application, and chemical pre-treatment on the yield and quality of nanosilica derived from rice husk (RH) and also comprehensively treats the effectiveness of H3PO4 pre-treatment on its structural and optical properties. Sample preparation involves chemical pre-treatment methods and calcination at 550 oC for 6 hours. The result shows that location and fertilizer application affects the yield and quality of silica derived from RH. H3PO4 pre-treatment proved to be very effective and improved both the structural and optical properties of the nanosilica, which is a potential candidate for solid-state lighting and display applications.

Corresponding Author:

C. Mbakaan,
Dept Department of Science Laboratory Technology,
Physics/Electronics Section,
Benue State Polytechnic, P.M.B. 01, Ugbokolo.
Email: celestinembakaan@gmail.com

1. INTRODUCTION

Due to the numerous applications of nanoscience and nanotechnology in practically all areas of human endeavor, particularly in the fields of energy and medicine, this topic is now the subject of intensive research. Recently, the research focus has shifted to rice husk (RH) as one of the major sources of silica [1–3]. The interest in rice husk is not only due to its rich silica content but also due to its availability and abundance in almost all parts of the world [4,5]. Besides, the husk is also very inexpensive across the globe [6–8]. The rich silica in rice husk especially when reduced to the nanoscale can be harvested for applications in Energy, medicine, agriculture, industries, and so on [9]. Typically, the nano-SiO_2 derived from rice husk is a major material for the synthesis of nanostructured silicon for high-performance Li-ion battery anodes [10,11], and solar cell fabrication [12]. It can also be explored for biomedical [13], chemical sensing [14] and ceramics [15], and so many other applications. Depending on the calcination temperature, the silica derived from rice husk exists in different forms as amorphous or crystalline silica. Rice husk produces 90 to 98 % amorphous silica when burnt at a controlled temperature of less or equal to 700 oC [16] in the case of untreated rice husk and short calcination time. Above the temperature of 700 oC, silica with negligible content of unburned

carbon is produced leading to crystallization [17]. For treated rice husk burnt at shorter times, the silica crystallizes at temperatures equal to or above 800 oC [18–21]. Different methods had been employed to synthesize silica from rice husks in the past decades. Most prominent among these methods include preparation from direct calcination of rice husk, preparation from post-treatment of rice husk ash, bio-method, and the sol-gel method [22–26].

The kind of application of silica derived from rice husk is highly dependent on the amount and quality of the derived silica. For instance, high-quality (pure silica of 99.999%) silica is required to produce the Nano-silicon needed for the fabrication of solar cells [12,27]. High-quality silica is also necessary to produce silicon for the fabrication of high-performance Li-ion battery anodes [10,28]. Very high-quality silica is also needed for most industrial and biomedical applications. However, the quality of silica derived from rice husk is dependent on many factors. Factors such as location, rice variety, fertilizer application, geographic and climatic conditions, calcination temperature, and synthesis method are key to deriving high-grade quality silica [29–31]. Though a detailed study has been done on silica derived from the husk of different rice varieties [8], most research attention has been shifted to the synthesis method as a factor to derive quality silica ignoring the other factors. Today, most researchers collect rice husk from milling stations just for deriving the silica without paying attention to other factors, resulting in several impurities in the silica. In addition, the synthesis method adopted by most researchers is the method of boiling rice husk in hydrochloric acid. The research report shows that even when rice husk is boiled in hydrochloric acid (HCl) several impurities still exist in the derived silica and the impurities can be further removed by soaking the HCl pre-treated husk in Phosphoric acid [8]. Although this has been studied and reported, a comprehensive study of the structural, morphological, optical, and other properties of Nano-silica prepared from rice husk through this route has never been studied and published to the best of our knowledge.

Given the above facts, herein, the research is aimed at an attempt to carry out a comprehensive study on the effect of factors such as location and fertilizer application on the quality of Nano-silica derived from rice husk. Furthermore, the structural and optical properties of the derived Nano-silica through phosphoric acid pre-treatment at three different concentrations are also studied in detail.

2.   Experimental
a.   Materials

Five samples of rice husk of Nerica-1 rice variety grown in five different locations in the Middle-belt of Nigeria, particularly Benue, Kogi, Nasarawa, Plateau, and Taraba states with and without fertilizer application were collected and used as the major raw material in this research. The samples from each state were labeled using the first letter of the name of the State as shown in Table 1.

Table 1: Sample label

Sample /State	Label
Benue	B1
	B2
Kogi	K1
	K2
Nasarawa	N1
	N2
Plateau	P1
	P2
Taraba	T1
	T2

B1, K1, N1, P1, and T1 are rice husk samples collected from Benue, Kogi, Nasarawa, Plateau, and Taraba States respectively. The rice husk samples are of the origin of the Nerica-1 rice variety that did not receive fertilizer application during growth. The samples B2, K2, N2, P2, and T2 are also from the same respective states and of the same Nerica-1 rice variety that receives fertilizer application during growth.

HCl (37 wt %; 99.9%), and H3PO4 (87 wt %) were purchased from Sigma Aldrich (Meck). No further purification was done and the products were used as received.

2.2   Preparation of nanosilica from rice husk using HCl/H$_3$PO$_4$ Acids.

Water pre-treatment was adopted for the treatment of samples for yield and quality of silica test. All the samples were sieved and washed thoroughly with deionized water. The washed sample of B1 was dried in an open space for 24 hours under a shield to drain the water content. The sample was then dried in an oven at 110 ºC for 24 hours. It was then calcined in a box furnace at a temperature of 550 ºC for 6 hours with a ramp rate of 10 ºC /min and allowed to cool to room temperature. The resulting silica from this B1 sample was labeled S: B1. The procedure was then repeated to obtain the remaining samples. All the samples were subjected to the yield test and the B1 sample collected from Benue State was later chosen as raw material for the preparation of nanosilica for further characterization including photoluminescence studies. The reason for the selection of this sample will become obvious from the yield result.

Acid (HCl/H_3PO_4) pre-treatment was done on sample B1 after thorough washing with deionized water following the same procedure reported in our previous articles [6, 7, 21]. Usually, 50g of dried B1 RH sample was mixed with 200 mL of 10 wt % hydrochloric acid (HCl). The mixture was boiled under constant stirring for 2 hours after which it was rinsed with deionized water to a neutral pH of 7. It was then pre-treated with phosphoric acid by soaking it in 0.8 M phosphoric acid (H_3PO_4) for 72 hours. Washing was then carried out to remove all the adherent acid particles to a pH of 7. It was then dried in an oven at 110 ºC for 24 hours and thereafter calcined in a box furnace for 6 hours at a temperature of 550 ºC with a ramp rate of 10 ºC /min. The produced nanosilica sample was allowed to cool to room temperature naturally and it was labeled RH-SiO2-0.8 M H_3PO_4. The procedure was repeated to produce nanosilica samples RH-SiO2-0.08 M H_3PO_4 and RH-SiO2-1.52 M H_3PO_4.

2.3   Characterization

The structures of the samples were determined by X-ray diffraction (XRD) using PANalytical X'Pert PRO with Cu Kα of wavelength 1.5406 nm. The morphology of the samples was obtained using Zeiss Auriga Field Emission Scanning Electron Microscope (FESEM) and Jeol JEM-2100 Transmission Electron Microscope (TEM), each equipped with energy dispersive X-ray spectroscopy (EDX) for chemical composition studies. The yield of the samples was also determined using X-ray fluorescence spectroscopy (XRF) model minipal4 pw425/45B © 2005 with Rh tube. Fourier Transform Infrared Spectroscopy (FTIR) was carried out using a Perkin-Elmer Ate-FTIR 100 spectrometer. The surface areas of samples were determined using the BET Surface area analyzer model Micromeritics TRISTAR II 3020. UV-Vis spectroscopy of the samples was obtained from Perkin-Elmer Lambda 1050 UV/Vis/NIR spectrophotometer equipped with an integrating sphere at room temperature Photoluminescence (PL) measurements were performed at room temperature using Hitachi F-7000 spectrophotometer.

3.0   Result and Discussion

3.1   Effect of Physical and chemical processing on the Yield and Quality of rice husk silica

The variety of rice, the temperature of calcination (incineration), holding time, and pre-treatment methods are reported to affect the quality of the silica from rice husk [8,32]. Besides, location and fertilizer application are also considered key factors for the production of high-yield and quality silica from rice husks. To determine the effect of location and fertilizer application on the yield and quality of silica from rice husk, the water pre-treatment method was deliberately adopted to avoid the total removal of most elements/compounds by acids while controlling other important factors. Table 2 presents the yield of silica from rice husks based on location and fertilizer application. The result shows a difference in yield based on the location. Though there is no significant difference in yield of silica from each state (location) based on fertilizer or no fertilizer application it shows an increase in the amount of K^+ and P where the plant receives fertilizer application during growth. The increase in the amount of K^+ and P has resulted in a decrease in the silica yield and quality irrespective of location indicating the strong influence of fertilizer application. Close observation reveals that some places have high silica yield even without fertilizer application more than even those with fertilizer application, confirming the effect of location on the quality and yield of silica. Most importantly, this result confirms that not only one factor plays a role in the grade and yield of silica and that the silica derived from rice husk irrespective of any pre-treatment method still contains several impurities. However, water pre-treatment is considered effective for the removal of most of the impurities. A comparison of this result with our previous result [8] confirms this as most impurities in the untreated sample in that result are not present in the result here indicating that they might have been removed due to the water pre-treatment. Therefore, it has become more apparent from the result in Table 2 that sample B1 because of the high silica and low K^+ and P content will be used throughout the remaining part of this research work and will be subjected to acid pre-treatment to further remove mineral impurities. Acid pre-treatment removes or reduce metal ion impurities particularly K^+ which promote the melting of RH-SiO_2 at relatively low temperature [25].

Table 2: Silica yields (%) of samples based on location and fertilizer application.

Compound	Major Element	Yield (%)									
		Benue		Kogi		Nasarawa		Plateau		Taraba	
		S: B1	S: B2	S: K1	S: K2	S: N1	S: N2	S: P1	S: P2	S: T1	S: T2
SiO$_2$	Si	91.60	86.56	87.93	84.14	89.20	88.99	86.96	86.05	89.70	89.30
P$_2$O$_5$	P	4.900	8.830	7.050	10.456	6.340	6.890	9.270	9.971	6.600	6.912
K$_2$O	K	1.900	3.461	2.826	3.920	2.616	2.498	2.233	2.764	2.000	2.254
CaO	Ca	0.930	0.610	0.956	0.731	0.914	0.875	0.988	0.799	0.887	0.663
Fe$_2$O$_3$	Fe	0.432	0.120	0.512	0.242	0.381	0.217	0.226	0.130	0.171	0.159
MnO	Mn	0.313	0.110	0.234	0.130	0.140	0.150	0.113	0.101	0.123	0.210
RuO$_2$	Ru	0.130	0.100	0.112	0.145	0.110	0.092	0.108	0.098	0.143	0.132
V$_2$O$_5$	V	0.002	0.001	0.002	0.012	0.011	0.010	0.017	0.015	0.042	0.033
TiO$_2$	Ti	0.100	0.060	0.130	0.016	0.022	0.031	0.021	0.016	0.025	0.018
ZnO	Zn	0.013	0.011	0.041	0.032	0.017	0.023	0.014	0.013	0.036	0.039
Re$_2$O$_7$	Re	0.016	0.004	0.003	0.021	0.032	0.041	0.002	0.001	0.045	0.061
Y$_2$O$_3$	Y	0.006	0.013	0.052	0.041	0.053	0.033	0.007	0.003	0.028	0.027
EuO$_3$	Eu	0.008	0.005	0.007	0.015	0.004	0.009	0.003	0.002	0.032	0.024
ZrO$_2$	Zr	0.012	0.018	0.021	0.016	0.029	0.032	0.020	0.018	0.037	0.030
CuO	Cu	0.034	0.043	0.046	0.032	0.058	0.063	0.013	0.010	0.077	0.067
Rb$_2$O	Rb	0.004	0.054	0.078	0.051	0.073	0.046	0.005	0.009	0.054	0.071

Table 3 presents the result of the chemical composition of nanosilica derived from HCl/H$_3$PO$_4$ Pre-treated Rice Husk. The result shows that HCl/H$_3$PO$_4$ pre-treatment removes most of the impurities including P$_2$O$_5$, V$_2$O$_5$, Y$_2$O$_3$, EuO$_3$, ZrO$_2$, and Rb$_2$O. The effectiveness of HCl/H$_3$PO$_4$ pre-treatment to remove impurities and improves the yield of silica and consequently, its quality has been reported [8]. It is also shown that H$_3$PO$_4$ is very effective in removing impurities that cannot be removed by HCl pre-treatment only [8], which is also confirmed in this work. The yield of silica in this work has risen to 99.61 % due to the further removal of more impurities. Most striking about this result is the complete removal of P$_2$O$_5$ and the reduction in the content of K$_2$O impurity from 1.90 % to 0.032 %. In addition, CaO and Fe$_2$O$_3$ have been reduced to the minimum by this method. Phosphoric acid has been reported to be very effective in the removal of iron from quartz sand [33].

Table 3: Chemical composition of nanosilica derived from HCl/H3PO4 Pre-treated Rice Husk

Compound	Major Element	HCl/H3PO4 Pre-treated Rice Husk Yield (%)
SiO$_2$	Si	99.61
K$_2$O	K	0.032
CaO	Ca	0.073
Fe$_2$O$_3$	Fe	0.103
MnO	Mn	0.015
RuO$_2$	Ru	0.109
TiO$_2$	Ti	0.032
ZnO	Zn	0.001
CuO	Cu	0.013
Re$_2$O$_7$	Re	0.012

Other factors which are known to influence the quality and yield of silica were also taken into consideration during the processing stage. The temperature of 550 °C was chosen because calcination at a relatively low temperature of 550 °C stops the formation of irregular aggregates by fusing [34]. The calcinations time of 6 hours is chosen to prepare amorphous and mesoporous silica nanoparticles (nanosilica) with a little amount of carbon.

3.2   Effect of H$_3$PO$_4$ Concentration on the Luminescence Properties of the RH Derived nanosilica.
3.2. 1 Structural Properties

The structural studies show that XRD patterns of RH-SiO$_2$ from HCl pre-treated RH soaked in higher concentrations of phosphoric acid (0.8 and 1.52 M) exhibit a single broad peak from 15 to 30° with a maximum at 2θ ~22.19° without any crystalline peak indicating purely-amorphous silica (Figure 33). However, the RH-SiO$_2$ pre-treated with low concentration (0.08 M) of phosphoric acid revealed several crystalline peaks at about 2θ = 20.88, 26.50, 36.56, 39.37, 42.45, 45.79, 50.00, 54.76, 59.79, 64.29, 68.206, 75.47, 81.63, and 83.89° which are assigned to (100), (101), (110), (102), (200), (021), (112), (202), (121), (113), (023), (302), (310), and (131) planes of quartz silica phase, respectively by JCPDS card no. 75-0443.
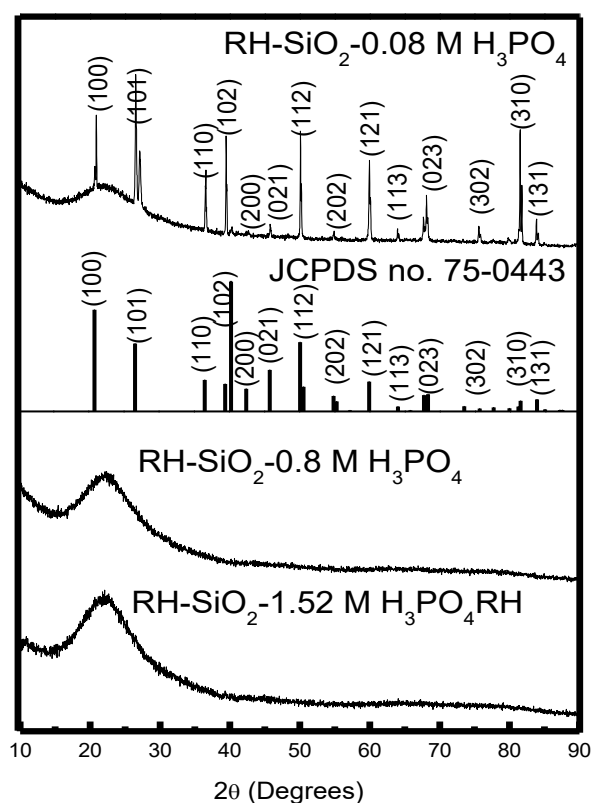

Fig 1: XRD patterns of RH-SiO$_2$ nanoparticles pre-treated with HCl and soaked in different concentrations of H$_3$PO$_4$.

The results here show that pure silica has been synthesized and that pre-treatment of RH with HCl and a high concentration of phosphoric acid can enhance the amorphous phase of silica after thermal treatment. The use of a lower concentration of phosphoric acid led to the crystallinity of the nanosilica as impurities particularly potassium may not have been significantly removed to stop the melting of the silica. Wang *et al.* [25] researched two samples of HCl-treated RH which were intentionally doped with Ca^{2+} and K$^+$ respectively. The Ca^{2+} and K$^+$ doped RH were calcined at 700 °C for 2 hours. After characterizations, the result showed that the K$^+$-doped RH led to the formation of semi-crystalline silica, while Ca^{2+}-doped RH produced amorphous silica. The melting effect of K$^+$ lowers the silica surface area, increases silica particle size, and is responsible for the encapsulation of impurities, which results in the crystallization of silica upon cooling to room temperature [25].

3.2.2   Microstructure, morphology, and chemical composition studies.

The FESEM images displayed in Fig.2 (a) and (b) show the formation of agglomerates of large and small irregular shape particles. Similarly, the TEM micrographs displayed in Fig. 2 (c) and (d) show the formation of nano-sized spherical-shaped particles. This is an indication that the agglomerated nanoparticles observed in the FESEM are indeed composed of spherical nanosilica. The TEM has a stronger penetrating power and so it is capable of detecting single particles. The average particle sizes of the particles presented in Table 4 as measured using the TEM micrographs gave values of approximately 30.4 and 43.1 nm for RH-SiO$_2$-0.8 M H$_3$PO$_4$ and RH-SiO$_2$-0.08 M H$_3$PO$_4$, respectively. The bigger particle size of the RH-SiO$_2$-0.08 M H$_3$PO$_4$ may be partly due to the melting effect of K$^+$ as earlier discussed. The insignificant effect of the K$^+$ ion due to its low content observed in Table 3 may partially have contributed to the small particle size observed in RH-SiO$_2$-0.8 M H$_3$PO$_4$.
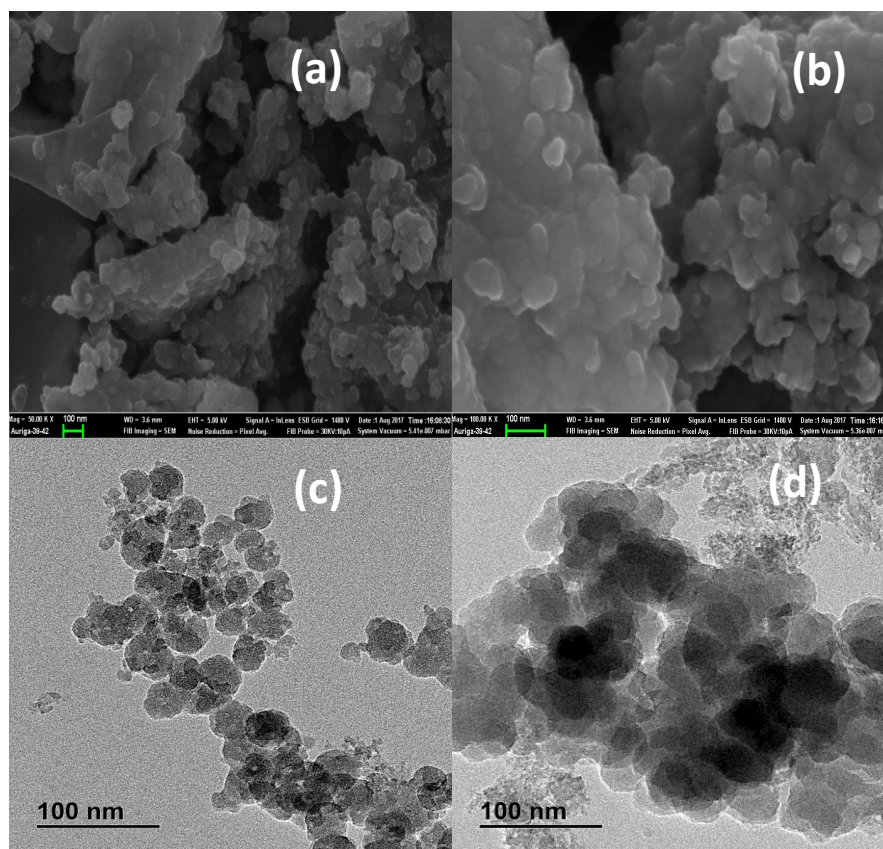
Fig 2 (a): SEM image of RH-SiO_2-0.8M H_3PO_4 (b) SEM image of RH-SiO_2-0.08M H_3PO_4 (c) TEM image of RH-SiO_2- 0.8M H_3PO_4 (d) TEM image of RH-SiO_2- 0.08M H_3PO_4

Table 4: Particle size analysis result of RH-SiO_2 derived from RH pretreated with HCl and H_3PO_4.

Sample	Particle size (nm)
RH-SiO_2-0.08 M H_3PO_4	43.089
RH-SiO_2-0.8 M H_3PO_4	30.385

The EDX results presented in Figures 3(a) and 3(b) show that RH-SiO_2-0.8 M H_3PO_4 (Fig. 3a) is composed mainly of Carbon (C), Oxygen (O), and silicon (Si) with sodium (Na) as an impurity which could not be detected with XRF, while RH-SiO_2-0.08 M H_3PO_4 (Fig.3b) is composed of Carbon (C), Oxygen (O) and silicon (Si). The Aluminium (Al) may be from the grid used in holding the sample since it was removed during acid pre-treatment.
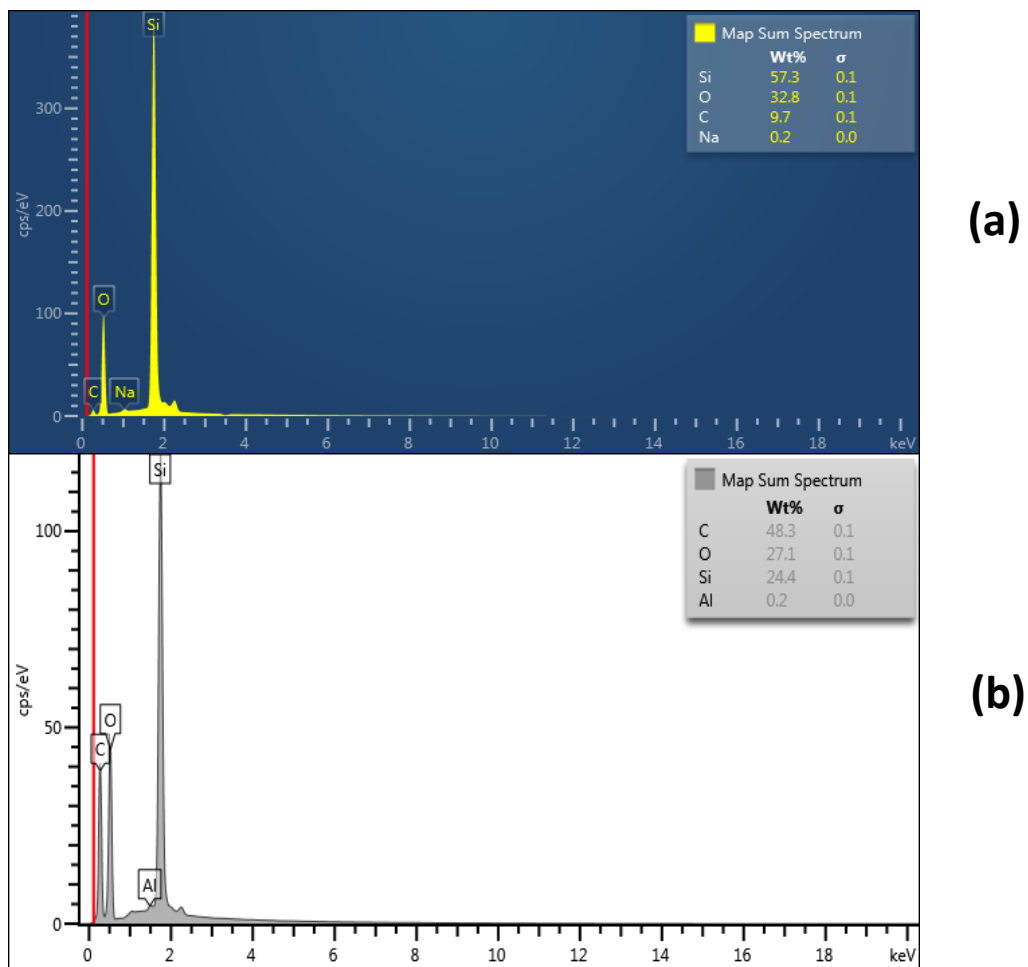
Fig 3: EDX of (a) RH-SiO$_2$- 0.8M H$_3$PO$_4$ (b) RH-SiO$_2$- 0.08M H$_3$PO$_4$

The results of EDX analysis in Figure 3 and presented in Table 5 further show that soaking HCl pre-treated RH in a higher concentration (0.8 M) of Phosphoric acid can provide the highest yield of nanosilica and significantly remove impurities. A low concentration of phosphoric acid does not enhance the yield of nanosilica and does not improve other properties of nanosilica derived from RH.

Table 5: EDX Result of RH pretreated with HCl and soaked in Phosphoric acid.

Element	Weight (%)	
	RH-SiO$_2$-0.8M HCl/H$_3$PO$_4$	RH-SiO$_2$-0.08M HCl/H$_3$PO$_4$
Si	57.30	24.40
O	32.80	27.10
C	9.70	48.30
Na	0.20	-
Al	-	0.2

3.2.3   Fourier transforms infrared (FT-IR) analysis.
Based on its excellent properties, RH-SiO$_2$-0.8 M H$_3$PO$_4$ was considered for FT-IR analysis.
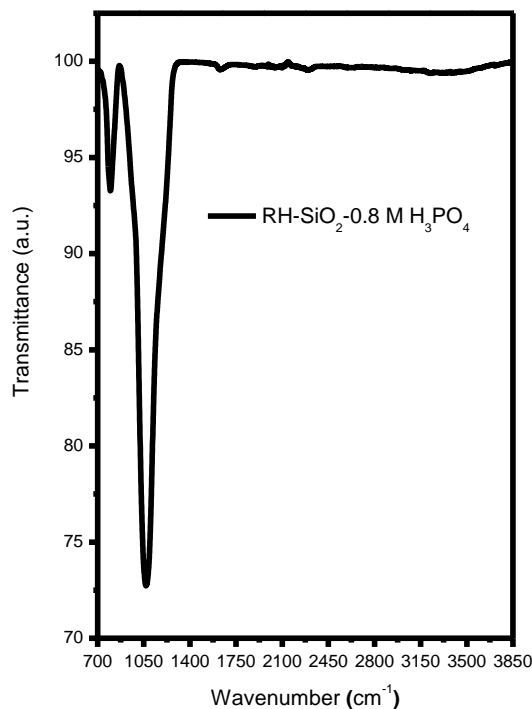
Fig 4: FT-IR spectra of RH-SiO$_2$-0.8 M, H$_3$PO$_4$ sample

Figure 4 (Fig.4) displayed the Fourier transform infrared (FT-IR) spectrum of the RH-SiO$_2$-0.8 M H$_3$PO$_4$. The FT-IR spectrum contains two absorption bands; a weak absorption band at ~795 cm^{-1} which is assigned to Si-O-Si symmetrical stretching vibrations [37–40], and a broad absorption band which is much stronger with a valley at 1068 cm^{-1}, assigned to the asymmetrical stretching mode of Si-O-Si [37–39,41]. There are weak bands with valleys at 1633 and 2309 cm^{-1} assigned to H-O-H bending mode and C=O bonds [40].

3.2.4   Surface area measurement

The result in Fig. 5 presented in Table 6 shows that the RH-SiO$_2$-0.8 M H$_3$PO$_4$ sample has 219.09 m^2/g, 0.25 cm^3/g, 4.57 nm, and 66.56 as surface area, BJH pore volume, pore size, and BET constant (C) respectively which indicates mesoporous silica. The result is comparable to the result of the work done by [42,43] and it indicates that soaking HCl pre-treated RH in phosphoric acid will effectively increase the surface area of the derived nanosilica. RH-SiO$_2$ derived from RH of Nerica -1 rice variety pre-treated with HCl only has been reported to have a surface area of 161.38 m^2/g [8] while the nanosilica derived from RH of Nerica-1 rice variety pre-treated with HCl/ H$_3$PO$_4$ in this research has an increased surface area of 219.09 m^2/g.
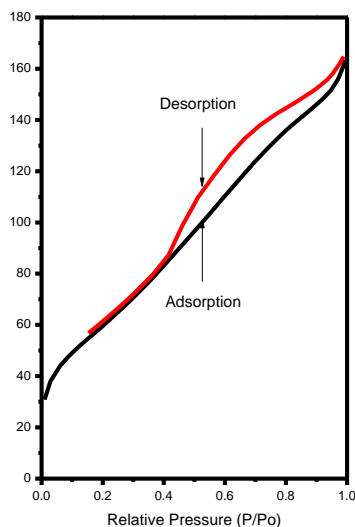

Fig 5: N$_2$ sorption isotherms of RH-SiO$_2$-0.8 M, H$_3$PO$_4$ sample

Table 6: Surface Area Measurement result of RH-SiO$_2$-Osi, RH-SiO$_2$-0.8M H$_3$PO$_4$, RH-SiO$_2$: 0.10 Sm^{3+}, and RH-SiO$_2$: 3 mol %Eu^{3+}.

Parameter	RH-SiO$_2$-0.8M- H$_3$PO$_4$
BET surface area (m^2/g)	219.09
BJH Pore volume (cm^3/g)	0.25
BJH Pore size (nm)	4.57
BET constant (C)	66.56

3.2.5   Optical Properties
Diffuse reflectance spectroscopy
The absorption bands (see Fig. 6a) are located at about 218, 249, and 319 nm for RH-SiO$_2$-0.08 M H$_3$PO$_4$.
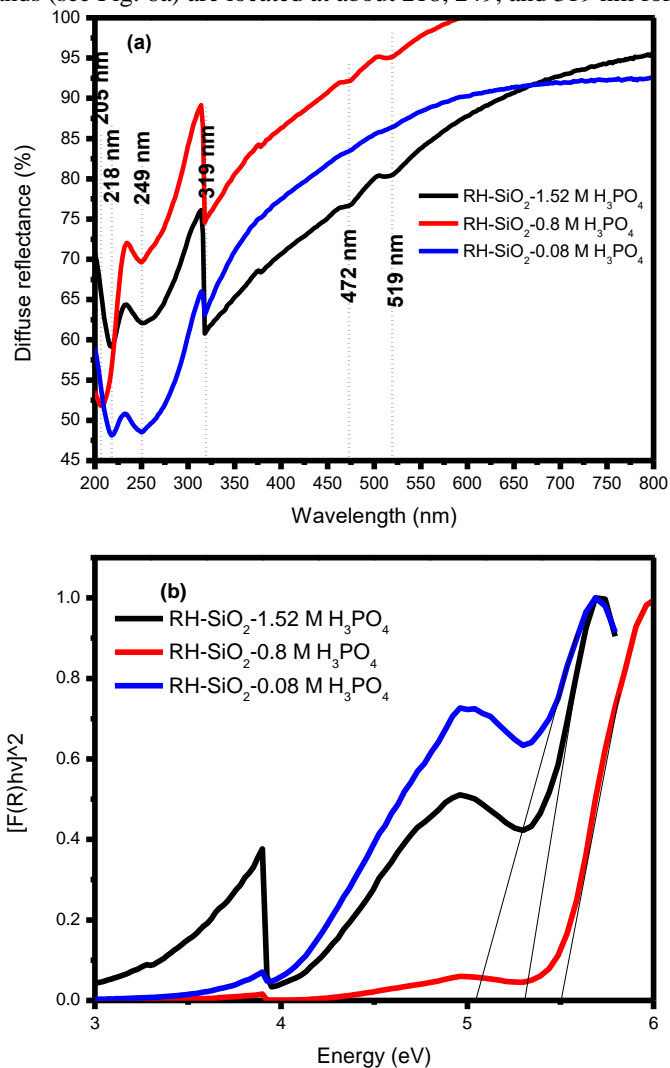

Fig 6: (a) Diffuse reflectance spectra and (b) Band gap of RH-SiO$_2$ nanoparticles derived from RH pre-treated with HCl/H$_3$PO$_4$.

It is observed that for RH-SiO$_2$-1.52 M H$_3$PO$_4$ the absorption bands are located at about 218, 249, 319, 472, and 519 nm while for RH-SiO$_2$-0.8 M H$_3$PO$_4$ the location of the absorption bands is similar to the previous sample except the 218 nm has been shifted to 206 nm. The absorption bands at 206 and 218 are band-to-band absorption of SiO$_2$. The bands at 249 and 319 nm are due to some defects centers such as oxygen deficiency centers in the SiO$_2$ [35]. The absorption bands at 472 and 519 nm are due to carbon impurities [36].
From Figure 6 (b), three sets of energies (absorption edges) 3.30 – 3.93, 3.93 – 5.31, and 5.31-5.80 eV could be observed from all the samples. The energy band gaps are located at about 5.03, 5.31, and 5.50 eV for RH-SiO$_2$-0.08 M H$_3$PO$_4$, RH-SiO$_2$-1.52 M H$_3$PO$_4,$ and RH-SiO$_2$-0.8 M H$_3$PO$_4$, respectively (Table 7) indicating

higher energy band for silica derived from RH samples pre-treated with a higher concentration of phosphoric acid.

Table 7: Band gap of RH-SiO$_2$ nanoparticles derived from RH pre-treated with HCl and phosphoric acid.

Sample	Band gap (eV)
RH-SiO2-0.08 M H$_3$PO$_4$	5.03
RH-SiO2-0.8 M H$_3$PO$_4$	5.50
RH-SiO2-1.52 M H$_3$PO$_4$	5.31

Photoluminescence studies

The photoluminescence excitation (PLE) spectra (Fig. 7) for RH-SiO$_2$-x H$_3$PO$_4$ where x= 0.08, 0.8 and 1.52 M samples obtained by monitoring emission at 435 nm show similar spectra which are broad with peaks at 221, 252, 275 and 365 nm.

The photoluminescence emission spectra of the RH-SiO$_2$-xH$_3$PO$_4$ (Fig. 8 (a)) under an excitation wavelength of 365 nm (Near UV light region) show continuous broad bands in the range 388-700 nm. The broadening is due to energy gap change in the SiO$_2$ or energy level increase as a result of the adjustment of the angle between Si-O-Si and inhomogeneous strain resulting from the substitution of Si by C [38]. The RH-SiO$_2$-0.8 M H$_3$PO$_4$ sample produced the strongest intensity (Fig. 8a) due to the increased purity of the samples. The deconvoluted spectrum (Fig. 8 (b)) of RH-SiO$_2$-0.8 M H$_3$PO$_4$ sample gave 5 Gaussian peaks with center at 411 nm (i) 431 nm (ii), 453 nm (iii), 483 nm (iv), and 528 nm (v). This result indicates that the nanosilica obtained by soaking HCl-pretreated RH in phosphoric acid gives emissions mainly in the blue (411, 431, 453, and 483 nm), and green (528 nm) regions of the visible spectrum.
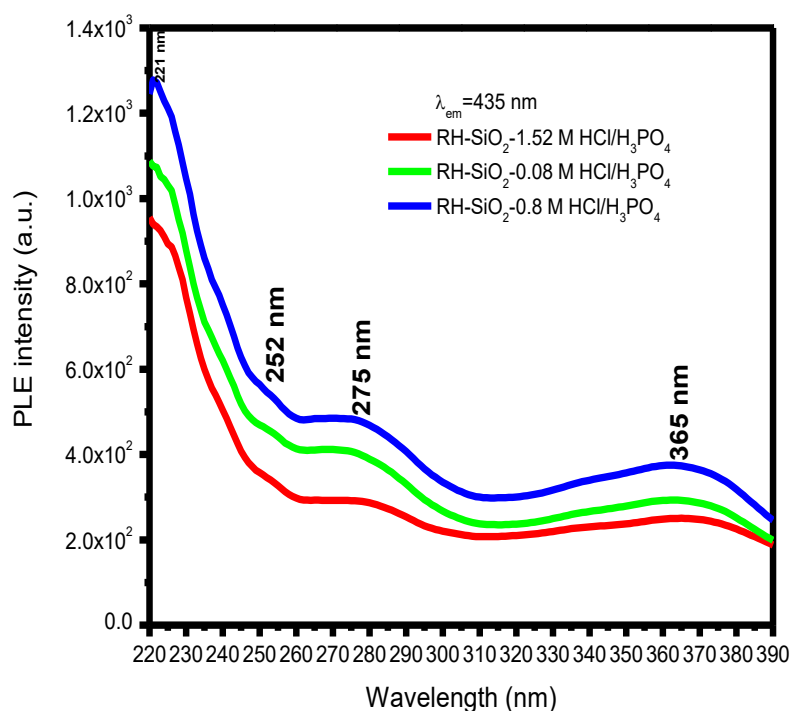

Fig 7: Excitation spectra of RH-SiO$_2$–x H$_3$PO$_4$ (x= 0.08, 0.8, and 1.52 M).

Like before, the emission peaks at 411, 431, and 453 are due to some defects centers in the silica such as oxygen-deficiency centers (ODCs), and non-bridging oxygen hole centers (NBOHC) etc [36] while the peaks at 483, 528 and 575 nm, are due to carbon impurities [36,42,44].

The result of Figure 9 presented in Table 8 shows the *Commission Internationale de I'Eclairage (CIE)* chromaticity diagram and coordinates respectively of emission spectra of RH-SiO$_2$-xH$_3$PO$_4$, (x= 0.08, 0.8, and 1.52 M) under 365 nm excitation. The coordinates show a shift to sky blue light as the concentration of the H$_3$PO$_4$ acid increased from 0.08 M to 1.52 M.
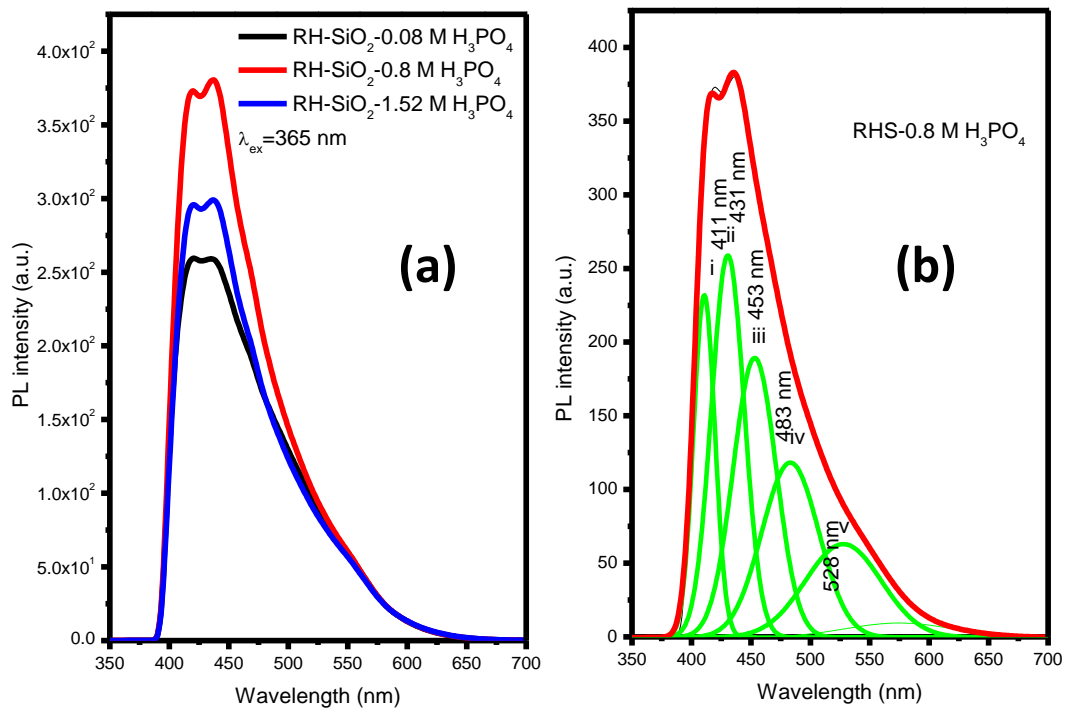
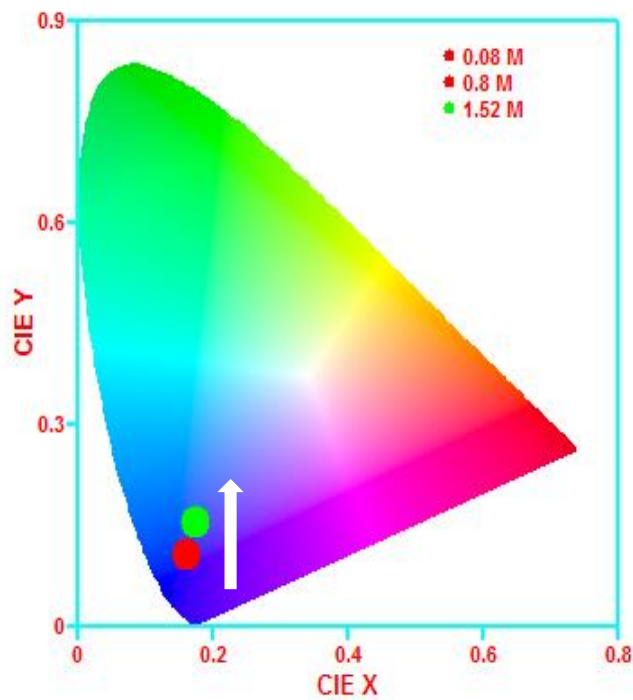Fig 8: (a) PL and (b) Deconvoluted spectra of RH-SiO$_2$–x H$_3$PO$_4$ (x= 0.08, 0.8 and 1.52 M)

Fig 9: CIE chromaticity coordinate diagram of RH-SiO$_2$ samples obtained from RH pretreated in HCl/H$_3$PO$_4$ (RH-SiO$_2$: xH$_3$PO$_4$ (x = 0.08, 0.8, 1.52 M).

Table 8: CIE chromaticity coordinates of RH-SiO$_2$ samples obtained from RH pre-treated with HCl/H$_3$PO$_4$ (λ_{ex}=365 nm).

RH-SiO$_2$ samples	*CIE* coordinates	
	x	y
RH-SiO$_2$ - 0.08M H$_3$PO$_4$	0.1604	0.1068
RH-SiO$_2$ - 0.8M H$_3$PO$_4$	0.1604	0.1068
RH-SiO$_2$ - 1.52 M H$_3$PO$_4$	0.1716	0.1547

4.0   Conclusion

The location of an area where rice is grown and fertilizer application has been shown to affect the yield and quality of silica derived from rice husk. Considering a particular location, the yield of silica is found to be high in areas where there is no fertilizer application, however, K$^+$ and other impurities content increase in areas of fertilizer application. Water pre-treatment and HCl pre-treatment of rice husk are confirmed capable of removing mineral impurities but pre-treatment of rice husk with HCl/H$_3$PO$_4$ is proved to be most effective in the removal of impurities thereby improving the quality of silica derived from rice husk. The HCl/H$_3$PO$_4$ pre-treatment method is also found to be very impressive in producing amorphous and mesoporous silica. The method generally improves the structural properties and enhanced the optical properties of the nanosilica derived from rice husk. The method is most successful when H$_3$PO$_4$ of higher concentration (0.8- 1.52 M) is applied. A lower concentration (0.08 M) is found to be weak and ineffective for most properties.

Conflict of Interest. The author has no conflicts to disclose.

Data availability. Data underlying the results presented in this paper are not publicly available at this time but may be obtained from the authors upon reasonable request.

REFERENCES

[1]   J. Chun, J.H. Lee, Recent progress on the development of engineered silica particles derived from rice husk, Sustain. 12 (2020) 1–19. https://doi.org/10.3390/su122410683.

[2]   N. Bisht, P.C. Gope, N. Rani, Rice husk as a fiber in composites: A review, J. Mech. Behav. Mater. 29 (2020) 147–162. https://doi.org/10.1515/jmbm-2020-0015.

[3]   Raphael Kungu, Paul Njogu, Robert Kinyua, Jackton Kiptoo, Green Chemistry Preparation and Characterization of Rice Husk Derived Silica Gel in Kenya, J. Environ. Sci. Eng. A. 8 (2019) 225–240. https://doi.org/10.17265/2162-5298/2019.06.001.

[4]   S.K.S. Hossain, L. Mathur, P.K. Roy, S.K.S. Hossain, L. Mathur, P.K.R. Rice, Rice husk / rice husk ash as an alternative source of silica in ceramics : A review, J. Asian Ceram. Soc. 6 (2018) 299–313. https://doi.org/10.1080/21870764.2018.1539210.

[5]   S.K.S. Hossain, P.K. Roy, Fabrication of sustainable insulation refractory: Utilization of different wastes, Bol. La Soc. Esp. Ceram. y Vidr. 58 (2019) 115–125. https://doi.org/10.1016/j.bsecv.2018.09.002.

[6]   M. Ahmaruzzaman, V.K. Gupta, Rice Husk and Its Ash as Low-Cost Adsorbents in Water and Wastewater Treatment, (2011) 13589–13613.

[7]   C. Mbakaan, I. Ahemen, A.N. Amah, A.D. Onojah, L. Koao, White-light-emitting Dy^{3+}-doped amorphous SiO$_2$ nanophosphors derived from rice husk, Appl. Phys. A Mater. Sci. Process. 124 (2018). https://doi.org/10.1007/s00339-018-2156-6.

[8]   C. Mbakaan, I. Ahemen, F.B. Dejene, A.D. Onojah, S.J. Motloung, R. Ocaya, A. Reyes-Rojas, A. Reyes-Rojas, Structural and optical properties of nano-SiO$_2$ derived from the husk of some rice varieties and the effect of doping with Sm^{3+} ions, Opt. Mater. Express. 11 (2021) 965. https://doi.org/10.1364/OME.419552.

[9]   P.G. Jeelani, P. Mulay, R. Venkat, C. Ramalingam, Multifaceted Application of Silica Nanoparticles. A Review, Silicon. 12 (2020) 1337–1354. https://doi.org/10.1007/s12633-019-00229-y.

[10]   N. Liu, K. Huo, M.T. McDowell, J. Zhao, Y. Cui, Rice husks as a sustainable source of nanostructured silicon for high performance Li-ion battery anodes, Sci. Rep. 3 (2013) 1–7. https://doi.org/10.1038/srep01919.

[11]   P. Jain, V. Fuskele, Rice Husk Ash as a Potential Source of Silicon and Its Varied Applications, SSRN Electron. J. (2020). https://doi.org/10.2139/ssrn.3529256.

[12]   S. Venkateswaran, R. Yuvakkumar, V. Rajendran, Nano Silicon From Nano Silica Using Natural Resource (RHA) for Solar Cell Fabrication, (2012) 37–41. https://doi.org/10.1080/10426507.2012.740106.

[13]   R. Konwar, A.B. Ahmed, Nanoparticle: an Overview of Preparation, Characterization and Application, Int. Res. J. Pharm. 4 (2013) 47–57. https://doi.org/10.7897/2230-8407.04408.

[14]   W. Pan, N.H. Wang, G.F. Li, G.L. Ning, Monodisperse, luminescent silica spheres synthesized by a new method, Mater. Sci. Forum. 675 677 (2011) 1093–1096. https://doi.org/10.4028/www.scientific.net/MSF.675-677.1093.

[15]   H. Chen, Biogenic silica nanoparticles derived from rice husk biomass and their applications, Texas State University, 2013.

[16]   A.A. Moosa, B.F. Saddam, Synthesis and Characterization of Nanosilica from Rice Husk with Applications to Polymer Composites, (2017). https://doi.org/10.5923/j.materials.20170706.01.

[17]   M.. Haslinawati, K. Matori, Z. Wahab, H.A. Sidek, A.. Zainal, Effect of Temperature on Ceramic from Rice Husk Ash, Int. J. Basic Appl. Sci. 9 (2009) 111–117. https://doi.org/10.1117/3.2315931.ch46.

[18]   R.A. Bakar, R. Yahya, S.N. Gan, Production of High Purity Amorphous Silica from Rice Husk, Procedia Chem. 19 (2016) 189–195. https://doi.org/10.1016/j.proche.2016.03.092.

[19]   E. Rafiee, S. Shahebrahimi, M. Feyzi, M. Shaterzadeh, Optimization of synthesis and characterization of nanosilica produced from rice husk (a common waste material), Int. Nano Lett. 2 (2012) 29. https://doi.org/10.1186/2228-5326-2-29.

[20]   J.S. Lim, Z. Abdul Manan, S.R. Wan Alwi, H. Hashim, A review on the utilization of biomass from rice industry as a source of renewable energy, Renew. Sustain. Energy Rev. 16 (2012) 3084–3094. https://doi.org/10.1016/j.rser.2012.02.051.

[21]   E. Rafiee, M. Khodayari, S. Shahebrahimi, M. Joshaghani, 12-Tungstophosphoric acid supported on nano silica from rice husk ash as an efficient catalyst for direct benzylation of 1,3-dicarbonyl compounds in solvent-free condition, J. Mol. Catal. A Chem. 351 (2011) 204–209. https://doi.org/10.1016/j.molcata.2011.10.008.

[22]   S.A. Abo-El-Enein, M.A. Eissa, A.A. Diafullah, M.A. Rizk, F.M. Mohamed, Removal of some heavy metals ions from wastewater by a copolymer of iron and aluminum impregnated with active silica derived from rice husk ash, J. Hazard. Mater. 172 (2009) 574–579. https://doi.org/10.1016/j.jhazmat.2009.07.036.

[23]   C. Mbakaan, I. Ahemen, A.D. Onojah, A.N. Amah, K.G. Tshabalala, F.B. Dejene, Luminescent properties of Eu 3 + -doped silica nanophosphors derived from rice husk, Opt. Mater. (Amst). 108 (2020) 110168. https://doi.org/10.1016/j.optmat.2020.110168.

[24]   H. Chen, W. Wang, J.C. Martin, A.J. Oliphant, P.A. Doerr, J.F. Xu, K.M. DeBorn, C. Chen, L. Sun, Extraction of lignocellulose and synthesis of porous silica nanoparticles from rice husks: A comprehensive utilization of rice husk biomass, ACS Sustain. Chem. Eng. 1 (2013) 254–259. https://doi.org/10.1021/sc300115r.

[25]   W. Wang, J.C. Martin, N. Zhang, Harvesting silica nanoparticles from rice husks, J. Nanoparticle Res. 13 (2011) 6981–6990. https://doi.org/10.1007/s11051-011-0609-3.

[26]   X. Ma, B. Zhou, W. Gao, Y. Qu, L. Wang, Z. Wang, Y. Zhu, A recyclable method for production of pure silica from rice hull ash, Powder Technol. 217 (2012) 497–501. https://doi.org/10.1016/j.powtec.2011.11.009.

[27]   J.A. Adebisi, J.O. Agunsoye, S.A. Bello, I.I. Ahmed, O.A. Ojo, S.B. Hassan, Potential of producing solar grade silicon nanoparticles from selected agro-wastes: A review, Sol. Energy. 142 (2017) 68–86. https://doi.org/10.1016/j.solener.2016.12.001.

[28]   K. Kaviyarasu, E. Manikandan, J. Kennedy, M. Jayachandran, M. Maaza, Rice husks as a sustainable source of high quality nanostructured silica for high performance Li-ion battery requital by sol-gel method - a review, Adv. Mater. Lett. 7 (2016) 684–696. https://doi.org/10.5185/amlett.2016.6192.

[29]   M.J. Kaleli, P.K. Kamweru, J.M. Gichumbi, F.G. Ndiritu, Characterization of rice husk ash prepared by open air burning and furnace calcination, J. Chem. Eng. Mater. Sci. 11 (2020) 24–30. https://doi.org/10.5897/jcems2020.0348.

[30]   B.I. Ugheoke, O. Mamat, A novel method for high volume production of nano silica from rice husk: Process development and product characteristics, Int. J. Mater. Eng. Innov. 3 (2012) 139–155. https://doi.org/10.1504/IJMATEI.2012.046898.

[31]   I.B. Ugheoke, O. Mamat, A critical assessment and new research directions of rice husk silica processing methods and properties, Maejo Int. J. Sci. Technol. 6 (2012) 430–448. https://doi.org/10.14456/mijst.2012.31.

[32]   S. Azat, A. V. Korobeinyk, K. Moustakas, V.J. Inglezakis, Sustainable production of pure silica from rice husk waste in Kazakhstan, J. Clean. Prod. 217 (2019) 352–359. https://doi.org/10.1016/j.jclepro.2019.01.142.

[33]   Z. Zhang, J. Li, X. Li, H. Huang, L. Zhou, T. Xiong, High efficiency iron removal from quartz sand using phosphoric acid, Int. J. Miner. Process. 114–117 (2012) 30–34. https://doi.org/10.1016/j.minpro.2012.09.001.

[34]   W. Wang, J.C. Martin, X. Fan, A. Han, Z. Luo, L. Sun, Silica nanoparticles and frameworks from rice husk biomass, ACS Appl. Mater. Interfaces. 4 (2012) 977–981. https://doi.org/10.1021/am201619u.

[35]   L.F. Koao, H.C. Swart, R.I. Obed, F.B. Dejene, Synthesis and characterization of Ce 3 + doped silica (SiO 2) nanoparticles, J. Lumin. 131 (2011) 1249–1254. https://doi.org/10.1016/j.jlumin.2010.10.038.

[36]   A.E. Abbass, H.C.S.R.E. Kroon, White luminescence from sol–gel silica doped with silver, J. Sol-Gel Sci. Technol. 76 (2015) 708–714. https://doi.org/10.1007/s10971-015-3825-y.

[37]   S. Duhan, P. Aghamkar, B. Lal, Influence of temperature and time on Nd-doped silica powder prepared by the solgel process, J. Alloys Compd. 474 (2009) 301–305. https://doi.org/10.1016/j.jallcom.2008.06.095.

[38]   Y. Ishikawa, S. Kawasaki, Y. Ishi, K. Sato, A. Matsumura, White photoluminescence from carbon-incorporated silica fabricated from rice husk, Jpn. J. Appl. Phys. 51 (2012). https://doi.org/10.1143/JJAP.51.01AK02.

[39]   L. Gong, H. Zou, G. Wang, Y. Sun, Q. Huo, X. Xu, Y. Sheng, Synthesis and luminescence properties of monodisperse SiO2@SiO2:Eu3+ microspheres, Opt. Mater. (Amst). 37 (2014) 583–588. https://doi.org/10.1016/j.optmat.2014.07.025.

[40]   Rachna Ahlawat, Synthesis and Characterizations of Europium doped Silica Nanophosphor., Int. J. Adv. Res. Sci. Eng. 6 (2017) 1077–1085.

[41]   C. Lin, Y. Song, F. Gao, H. Zhang, Y. Sheng, K. Zheng, Z. Shi, X. Xu, H. Zou, Synthesis and luminescence properties of Eu(III)-doped silica nanorods based on the sol-gel process, J. Sol-Gel Sci. Technol. 69 (2014) 536–543. https://doi.org/10.1007/s10971-013-3254-8.

[42]   Y. Liu, Z. Wang, H. Zeng, C. Chen, J. Liu, L. Sun, W. Wang, Photoluminescent mesoporous carbon-doped silica from rice husks, Mater. Lett. 142 (2015) 280–282. https://doi.org/10.1016/j.matlet.2014.12.034.

[43]   Z. Wei, Z. Wang, W.R.T. Tait, M. Pokhrel, Y. Mao, J. Liu, L. Zhang, W. Wang, L. Sun, Synthesis of green phosphors from highly active amorphous silica derived from rice husks, J. Mater. Sci. 53 (2018) 1824–1832. https://doi.org/10.1007/s10853-017-1637-x.

[44]   Z. Wang, S. Zeng, Y. Li, W. Wang, Z. Zhang, H. Zeng, W. Wang, L. Sun, Luminescence Mechanism of Carbon-Incorporated Silica Nanoparticles Derived from Rice Husk Biomass, Ind. Eng. Chem. Res. 56 (2017) 5906–5912. https://doi.org/10.1021/acs.iecr.7b00700.